UNIVERSITI PUTRA MALAYSIA

MICROSTRUCTURES OF YBCO THIN FILMS GROWN BY PLD

NUR DANISHA ANUM BINTI AMINUDIN

MICROSTRUCTURES OF YBCO THIN FILMS GROWN BY PLD

by

NUR DANISHA ANUM BINTI AMINUDIN

A Thesis submitted to
Universiti Putra Malaysia
For the degree of
BACHELOR OF SCIENCE WITH HONOURS IN INSTRUMENTATION SCIENCE

ABSTRACT

Three YBCO films – MGD001, MUSTO30 and MYB06 undergo three different mechanisms which are Atomic Force Microscopy (AFM), Energy Dispersion X-ray (EDX) and X-ray Diffraction. It is found that there is a difference between a pure YBCO coated film and one that has different compositions in it.

DEDICATION

I dedicate this work to my supervisor, Assoc. Prof. Dr. Mohd Mustafa Awang Kechik for the guidance and being patient with me throughout my journey. Kak Nabilah Abdullah for being attentive and showed the ropes on submitting the samples to the lab for characterization. Izyan Fatihah – for coming in with a clutch, helping out during my desperate times. Thank you, everyone.

ACKNOWLEDGMENTS

I would like to thank God for getting me through the two semesters I had to face whilst doing this research – physically, mentally, emotionally, financially. Words can't describe of how proud I am with myself with the impossible. Special thanks to my parents, family and friends. I couldn't have gone through it all without the help of those around me. I know this may not be the best one out there but it's definitely an experience I'm bound to remember in years to come. To the ones reading this, I hope whatever challenges you're facing, you'll find the strength in you to hang on and have faith in whatever you believe in – God, any higher spiritual being or yourself. You can do it. I believe in you.

TABLE OF CONTENTS

LIST OF FIGURES

LIST OF TABLES

LIST OF ABBREVIATIONS

[If appropriate. Click and insert list of abbreviations and/or definitions. Do not number this page or record it in the table of contents.]

Chapter 1

INTRODUCTION

1.1 Background of Study

Mankind has gone far with technological advancements in recent years. If we were to compare the amount of energy used to carry out daily tasks back then and now, it would be impractical as a result. At first, we started off ith the discovery of electricity which made things a lot easier since then. After quite some time, superconductors came into the picture. Kamerlingh Onnes discovered superconductivity in 1911 (Luiz, 2011). Superconductivity has been a significant contribution to theoretical physics. In 1935, F. London gave the first successful set of phenomenological equations for superconducting metals. Practical methods are improving steadily as the years go by. The BCS theory was the first successful theory that explained the microscopic mechanisms of superconductivity in metals and alloys.

An example that can be used for said theory is a thin film. A thin film is a layer of material ranging from a fragment of a nanometer (monolayer) to several micrometers in thickness. When thin films have high surface-to-volume ratios, the reaction for each film varies. This statement is valid as long as the thin film is from the same chemical composition. Films that are hard due to anti-abrasiveness under contact sliding, as well as those that are anti-abrasive to operating conditions, are characterized as hard thin films.

1.2 Importance of Study

Characterization is a diverse field. One of its importance is measuring a material's property allows experimental improvement in the property. In addition, making unique measurements improves the differentiation in specific areas. In this case, different values of critical temperature for each $YBa_2Cu_3O_7$ thin film carry a significant meaning of its own relating to its properties. Furthermore, characterization is a method that studies the compositional and structural origins of material in depth.

In general, the highest T_c accepted in the scientific literature is roughly equivalent to 135 K at 1 atm in the Hg-Ba-Ca-Cu-O system (Schilling & Cantoni, 1993). However, T_c can increase up to 180 K by adding external forces onto the system. It is believed that room temperature superconductor is possible only when the microscopic mechanisms of oxide superconductors have been clarified.

A microscopic theory takes the surface excess free energy as a function of the volume fraction profile near the surface, $\phi(z)$, and finds the profile that minimizes the surface excess free energy. The BSC theory is a chemical interaction between electrons in the solid that overcomes their normal electrostatic repulsion. Therefore, forming bound pairs is known as Copper pairs. It was found that the charge of particles carrying supercurrent is twice the charge during pre-existence BCS theory. The theory explained how vibrating atoms in a lattice caused electrons to form bound pairs. A phonon is a lattice vibration wave that moves through the lattice in the phonon mechanism of a Copper pair formation. Outer valence

electrons are detached and delocalized due to the positively charged atoms of the metal lattice, thereby becoming part of the conduction process.

1.3 Problem Statement

Thin films have a more comprehensive range of potential applications than other materials, thus becoming a major research field. Although previously mentioned that superconductors containing oxide (discovered in) as one of its components is ideal and critical temperature could be acquired just as easily, obtaining the data depends on the stability of the content itself. The thin films have been kept for a decade in an enclosed container at cooling temperature. This research is carried out to find out whether the time is related to the superconductivity properties of thin films. The method used to measure the thin films are by using X-ray Diffraction (XRD), Scanning Electronic Microscope (SEM) and Atomic Force Microscopy (AFM).

1.4 Objectives of the Project

The purpose of this research is based on the following objectives :

1) To observe the post annealing effect of thin films within a period of time.
2) To determine microstructural and morphological properties of thin films.

Chapter 2

LITERATURE REVIEW

2.1 Introduction

Normal conductors are made from a material that can conduct electricity if electrons, carriers of a negative charge, move through it when they experience a force. An electric field arising from a voltage applied across the conductor provides the force. However, not all solids are good electrical conductors. Copper is an excellent example of an electrical conductor since it is commonly used in electrical wires. The ability of a material to conduct electricity is measured by its resistivity, R. A material that has low resistivities is considered a good conductor, while one that has a significant value of resistivity is regarded as poor conductors.

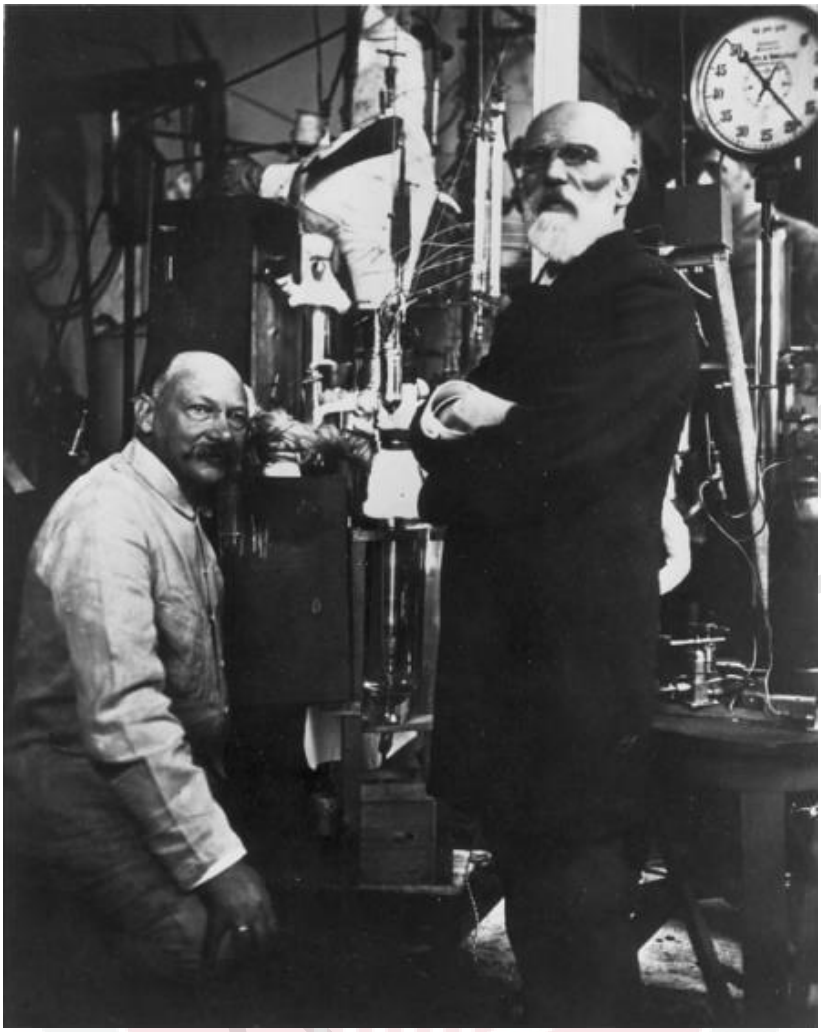

Picture 1. Heike Kamerlingh Onnes and J. D. van der Waals pose in 1911 in front of the helium liquefier developed by Onnes. The figure behind the pressure gauge (upper right corner) is unidentified (G. Holst? G. J. Flim?). (Kamerlingh Onnes Laboratory, Leiden. Courtesy of Caltech Archives, Earnest Watson Collection) (Goodstein & Goodstein, 2000).

2.2 History of superconductivity

During ancient times, humankind relied on sunlight and nature to generate power in their daily lives. Tasks as simple as mowing, laundry and cooking required a significant amount of time and energy to get them done. After electricity came about, tasks could be carried out quickly as well as time and energy conserving. Electricity is a type of power that needs to be

generated. Although life became more easygoing for humankind, it was insufficient to carry out more significant tasks like construction and mass agriculture. Therefore, superconductors are invented. A superconductor is a material that can conduct electricity or transport electrons from one atom to another with no resistance. Superconductivity is a phenomenon that occurs at very low temperatures. To put in simpler terms, no heat, sound, or other form of energy would be released from the material when it reached "critical temperature" (T_c) (Cheng, 1949).

Superconductors are also the first macroscopic quantum systems to seek practical applications. The main utilization in everyday life include generating high magnetic fields, such as in MRI systems that are used in hospitals, and filtering radio signals in particular in base stations of mobile telephony networks. Superconductivity is also implemented in ultra-sensitive magnetic field and temperature sensors, ultra-low noise amplifiers and as well as basic elements of quantum computers are being currently developed (Cheng, 1949).

2.3 General Properties of Superconductivity

One of the properties of superconductors is their critical temperature (T_c) or also known as transition temperature. The critical temperature is when the material changes from conductors to superconductors at a specific temperature. The transition is sudden and thorough. Superconductors have little to no resistance. When the temperature of the material is reduced below the critical temperature, its resistance reduces to zero. An example would be mercury that shows zero resistance below 4 Kelvin .

An electric field in a metal produces a current. Ohm's Law relates the current density and the electric field:

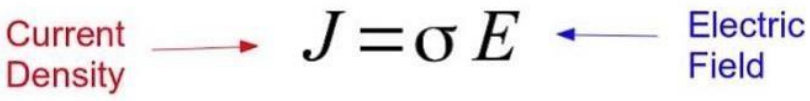

Equation 1

where σ is the electrical conductivity. Electrical resistivity ρ is the reciprocal of conductivity. The charge carriers in metals are electrons in conduction bands, which are partially energy bands, so they are called conduction electrons. Resistance of electrical conduction in metals is caused intrinsically by collisions between electrons and discrete vibrational modes in crystal lattices (phonons) and extrinsically by collisions between conduction electrons and imperfections as well as impurities in the crystal lattice (Siegrist et al., 1991). The resistances from these types of crashes are mainly independent of each other.

2.3.1 Type I and Type II Superconductors

The dissimilarity between type I and type II superconductors can be found in their magnetic behaviour. A type I superconductor is in its superconducting state until a required applied field H_c is reached. Any value beyond that no longer matters. A type II superconductor will only keep out the magnetic field out until a first critical field H_{c1} is reached. Vortices start to appear afterward. A magnetic flux quantum that penetrates the superconductor is called a vortex; where the vortex appears, the superconducting order parameter drops to zero. The metal is no longer a superconductor in this region. A current starts to circulate around the vortex. Even though the vortices have been formed, the other parts of the metal stay in a superconducting state. If the field is increased to the second critical field H_{c2}, the superconducting state of the metal comes to an end. H_{c2} usually has a more significant value than H_c, so type II superconductors are typically used for superconducting magnets.

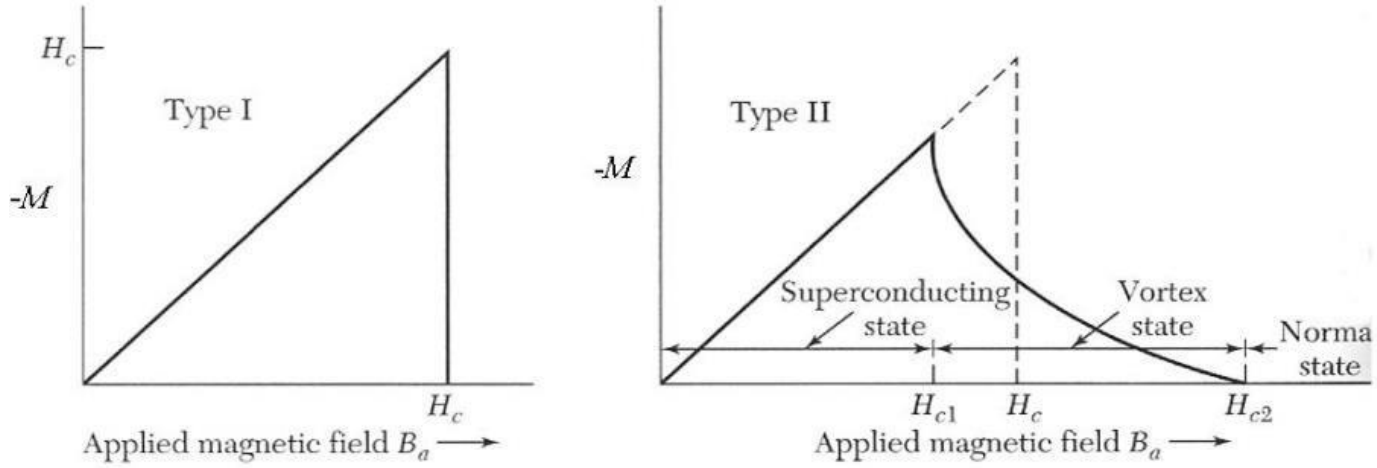

Figure 0.1. Magnetization of type I (left) and type II (right) superconductors depending on the applied field (Orthacker, n.d.)

Figure 1.1 illustrates the difference in the magnetic behaviour of type I and types II superconductors. As B~ = μ0(H~ + M~) (1) −M~ = H~ means that the whole field is kept out. If −M < ~ H~ not the whole field is kept out anymore. In a type I superconductor the coherence length ξ (length over which superconductivity changes) is bigger than the penetration depth λ (B~ = B~ 0 ∗ exp(x/λ)~ez). The coherence length is shorter than the penetration depth in a type II superconductor. Therefore, it is favourable for vortices to form. An example of a type II superconductor being applied is the Maglev train.

2.3.2 Maglev train

The innovation in transportation is a result of the increase of population and expansion in living areas. Slow mass transit becomes unreliable as the demand for faster transportation increases. In addition, the transport is expected to be convenient, eco-friendly, light-weight,

time-conserving. The magnetic levitation (Maglev) train is one of the best examples that meets the said requirements.

The revolutionary Maglev train technologies are investigated. Fig. 1 represents the difference between the conventional train and the Maglev train. The conventional train uses a rotary motor for propulsion and relies on the rail for guidance and support whereas the Maglev train gets propulsion force from a linear motor and utilizes electromagnets for guidance and support (Lee et al., 2006).

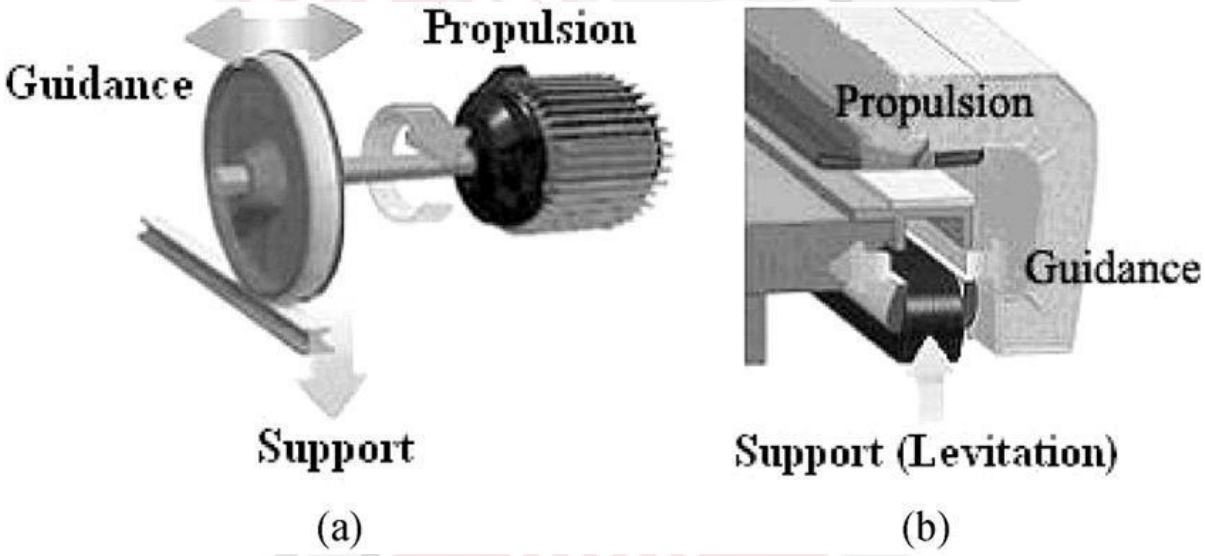

Fig. 1. Comparison of support, guidance, and propulsion. (a) Wheel-on-rail system. (b) Maglev system (Lee et al., 2006)**.**

Microstructure studies on YBCO films is crucial here. Need more to be added.

Chapter 3

METHODOLOGY

3.1 Introduction

A great deal of effort was put into the research of determining the characterization of particle size effect on the superconducting properties of $YBa_2Cu_3O_{7-x}$ particles. One of the many mechanisms that were carried out is related to its critical temperature, Tc. Therefore, experiments have been carried out to find out the effectiveness of $YBa_2Cu_3O_{7-x}$ after a decade has passed. XRD, AFM and SEM methods are used to obtain the desired results throughout the process. A variety of superconducting thin films exist. However, only 4 types were chosen: MUSTO24, MUSTO30, MGD001 and MYB06.

3.2 High-Temperature Superconductors

In 1986, J. G. Bednorz and K. A. Müller reported that the metal oxide ceramic $La_{2-x}Ba_xCuO_4$ becomes a superconductor above 30 K which lead them to win the Physical Noble prize the following year. The compound Nb_3Ge had the highest critical temperature of 23.2 K before then. The superconductivity of $La_{2-x}Ba_xCuO_4$ was the turning point of

research on a new family of materials referred to as high-temperature superconductors. M. K. Wu et al. discovered that another copper oxide $YBa_2Cu_3O_7$ (YBCO) is superconducting with a critical temperature of 92 K. YBCO was the first superconductor that seemed to have a critical temperature above the boiling point of nitrogen at 77 K.

La was replaced by Y and gave rise to $YBa_2Cu_3O_{7-x}$ (YBCO) that exhibited a T_C of ~92 K as first shown by Wu and his students at University of Alabama, Huntsville in 1987 (Akmaliyah, 2013). It is proven that the materials obtain the highest T_C value when the materials are slightly oxygen deficient i.e. when x = 0.15. Superconductivity decreases at x ˜ 0.6, when structure of YBCO changes from orthorhombic to tetragonal. Many other oxides such as thallium and mercury based oxide compounds expressed an even higher transition temperatures and these are commonly known as type II superconductors.

Compound		**T_c (K)**	**Crystal structure**
Y-based	$YBa_2Cu_3O_7$	92	Orthorhombic
Bi-based	$Bi_2Sr_2CuO_6$	20	Tetragonal
	$Bi_2Sr_2CaCu_2O_8$	85	Tetragonal
	$Bi_2Sr_2Ca_2Cu_3O_6$	110	Tetragonal
Tl-based	$Tl_2Ba_2CuO_6$	84	Tetragonal
	$Tl_2Ba_2CaCu_2O_8$	108	Tetragonal
	$Tl_2Ba_2Ca_2Cu_3O_{10}$	125	Tetragonal
	$TlBa_2Ca_3Cu_4O_{11}$	122	Tetragonal
Hg-based	$HgBa_2CuO_4$	94	Tetragonal
	$HgBa_2CaCu_2O_6$	128	Tetragonal
	$HgBa_2Ca_2Cu_3O_8$	134	Tetragonal

Figure 0.1. List of important oxide superconductors is shown below with their structures and transition temperatures (*Module 7: High Temperature Superconductors Introduction*, 2012)

The high-temperature superconducting materials are under Type–II superconductors and gradual change can be seen in transition temperature as a function of the magnetic field. In-depth research on developing a theory for high temperature superconductivity has been carried out and thus, a few mechanisms have been proposed. The first mechanism is based on the anti-ferromagnetic spin fluctuations in a doped system like cuprates. Spin fluctuation tests yield information on the symmetry of the pairing wave function which, for cuprates, should be of the type dx^2-y^2. The second model is the interlayer coupling model which states that superconductivity in a layered structure consisting of BCS-type symmetry i.e. s-wave symmetry can be enhanced without needing external force. Unfortunately, both of these models do not entirely explain the high temperature superconductivity.

3.3 $YBa_2Cu_3O_{7-x}$

The crystal structure of $YBa_2Cu_3O_{7-x}$ ("Y123") is characterized by the arrangement of copper-oxygen planes and copper-oxygen chains. The assembling sequence of YBCO layers along the crystal's c-axis goes as follows: CuO – BaO – CuO_2 – Y – CuO_2 – BaO. CuO_2 planes containing yttrium atoms between the copper-oxygen planes is detached the perovskite structure layers of YBCO. Oxygen atoms bridge a square lattice of copper atoms to form the planes. CuO chains run parallel to the copper-oxygen planes, with barium atoms sandwiched between them. Figure 1 depicts the unit cell of $YBa_2Cu_3O_{7-x}$.

Changing the oxygen concentration of $YBa_2Cu_3O_{7-x}$ altered its physical properties as a result. According to numerous research, it is significant that the critical temperature and crystal structure of $YBa_2Cu_3O_{7-x}$ change with oxygen content. Neutron diffraction and magnetic measurements have shown that T_c is dependent on the charge balance between the copper-oxygen chains and copper-oxygen planes. The chain sites serve as charge reservoirs from which electrons are transferred to the copper-oxygen planes as the oxygen content decreases. The superconductivity of the copper-oxygen planes resides within. As the oxygen content of $YBa_2Cu_3O_{7-x}$ decreases so does T_c. The material goes through a structural change and the material's superconductivity disappears when the oxygen content is below 6.3. [(Siegrist et al., 1991)]

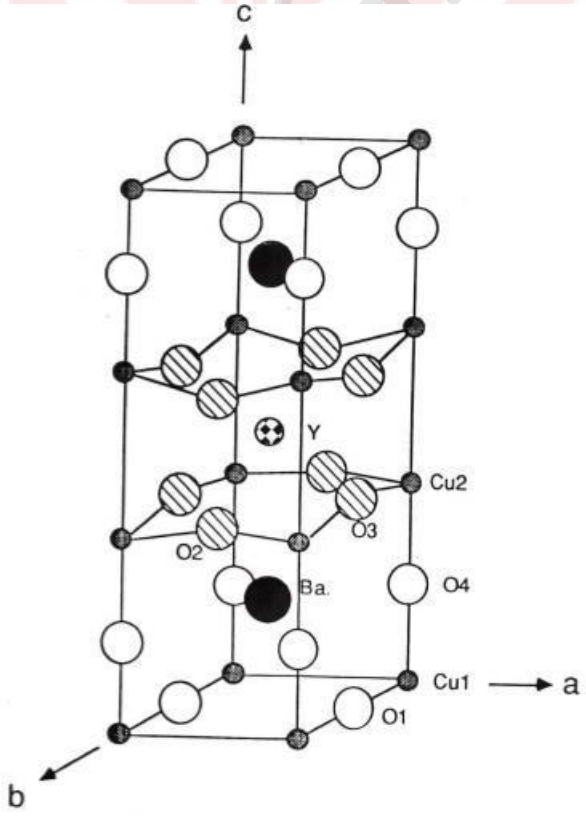

Figure 1 : Crystal structure of $YBa_2Cu_3O_7$ (Siegrist et al., 1991)

The samples used in this project are MUSTO30, MGD001 and MYB06. These three samples are YBCO samples. However, only MGD001 is not considered as pure YBCO because it is a thin film that has been mixed with Gd2411 as single layer growth. Move all this part to chapter 2

Chapter 4

RESULTS AND DISCUSSION

4.1 Introduction

Three types of characterization was carried out in this project to obtain its objectives which are AFM, SEM and XRD. The main purpose is to observe the microstructure degradation of the samples such as the surface roughness and grain size by using Atomic Force Microscopy (AFM). Scanning Electron Microscopy (SEM) provides high-resolution imaging to identify any surface fractures, flaws, contaminants or corrosion. To determine the underlying crystal structure of a material, X-Ray Diffraction (XRD) is also used. It enables the verification of the crystallinity and structure of a sample. However, no information on the sample's chemical nature. The topography of the samples is observed using Fields Emission Scanning Electron Microscopy (FESEM).

The YBCO films are highly sensitive to deposition conditions. The deposition parameters such as deposition temperature (T_s), deposition oxygen pressure and annealing

oxygen pressure (O_{ap}) affect the level of quality films obtained. All the films are fabricated by Pulsed Laser Deposition (PLD) to polish the films and get rid of any unwanted substances. The samples then go through the annealing process. The results obtained are from the pre-annealing and post-annealing processes. This is to present what changes occur before and after heating of samples.

4.1 Atomic Force Microscopy Analysis

Below are shown AFM images of YBCO thin film at a different dimension where, Figure (a) two dimension and (b) three dimension respectively. The grain boundary distributions are close to each other which are highly homogenous, as shown by the scanned image. Each sample is measured with scan size 2.00 µm and scan rate 2.40 µm/s. Elaborate more on surface roughness and surface growth such as spiral or island growth. Need more supporting statements from other people (literature) who are doing the same films. How the pure film look like? Get some paper to discuss.

4.1.1 Images of The Result

a)

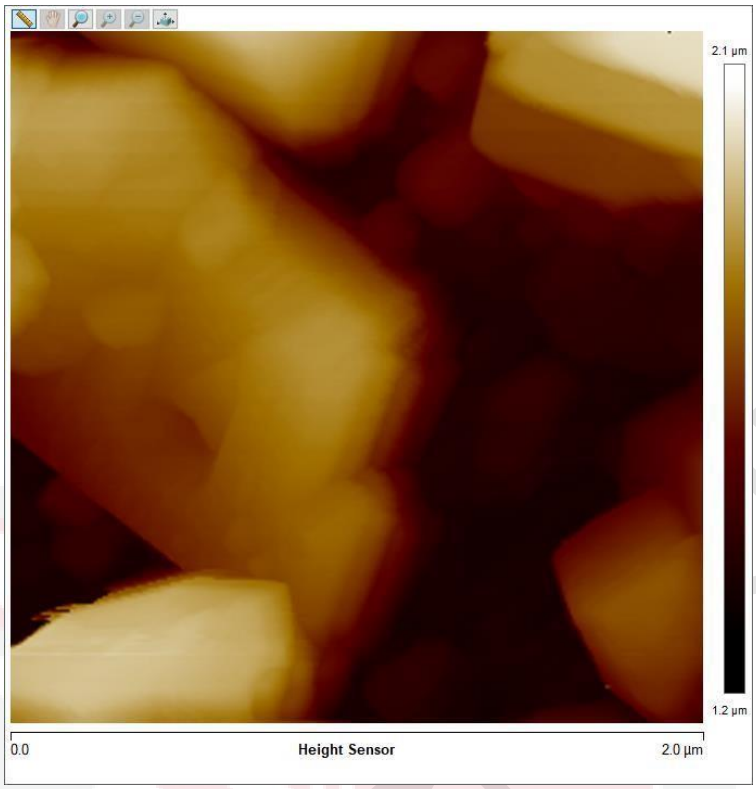

b)

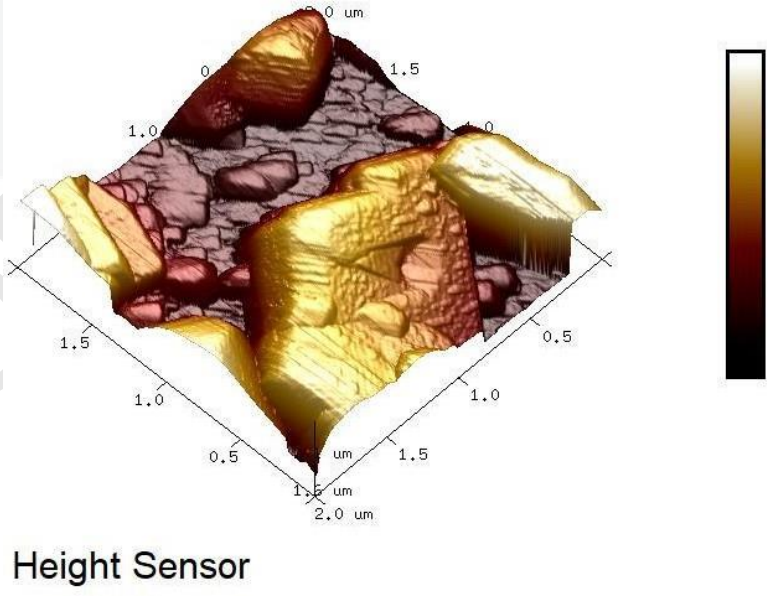

Figure 4.1. AFM images of MGD001 film at different dimensions with high distribution with a peak width 649 nm. a) 2D b) 3D

Based on Figure 4.1, the image was captured on MGD001 where the steps from high region have lighter tone than the lower region with a darker tone of colour.

a)

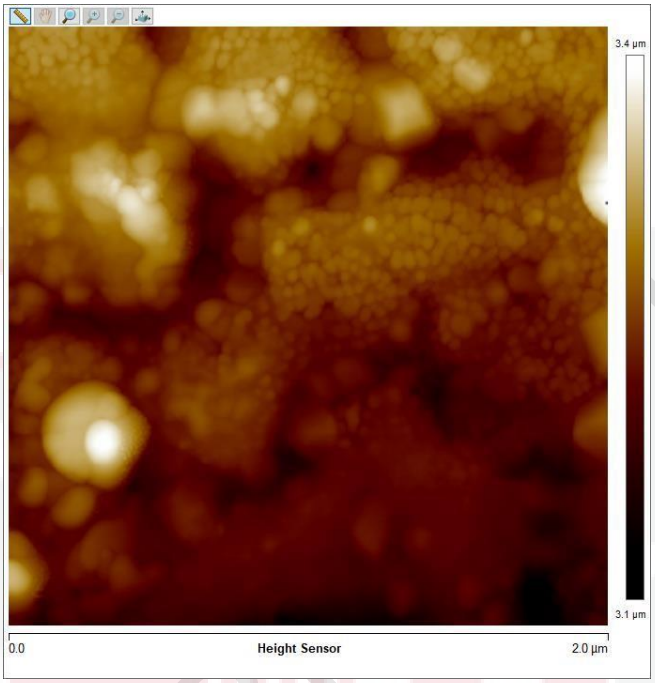

b)

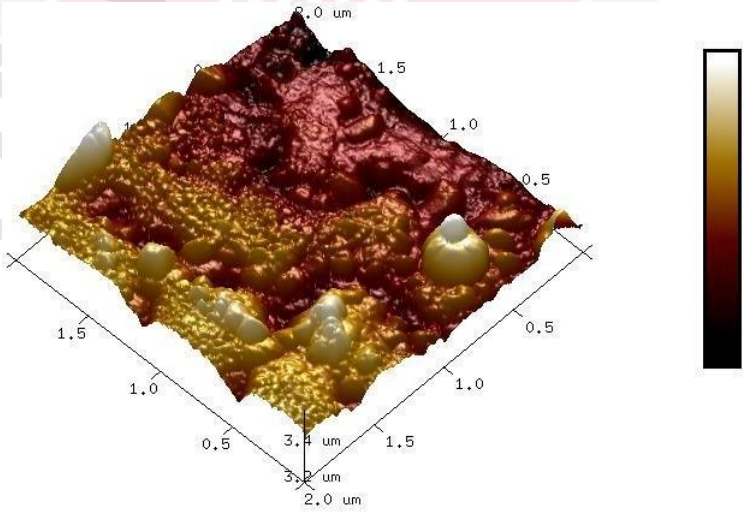

Figure 4.2. AFM images of MUSTO30 film at different dimension with high distribution with a peak width of 178 nm. a) 2D b) 3D

Based on Figure 4.2, the image was captured on MUSTO30 where the steps from the high region have a lighter tone than the lower region with a darker tone of colour.

a)

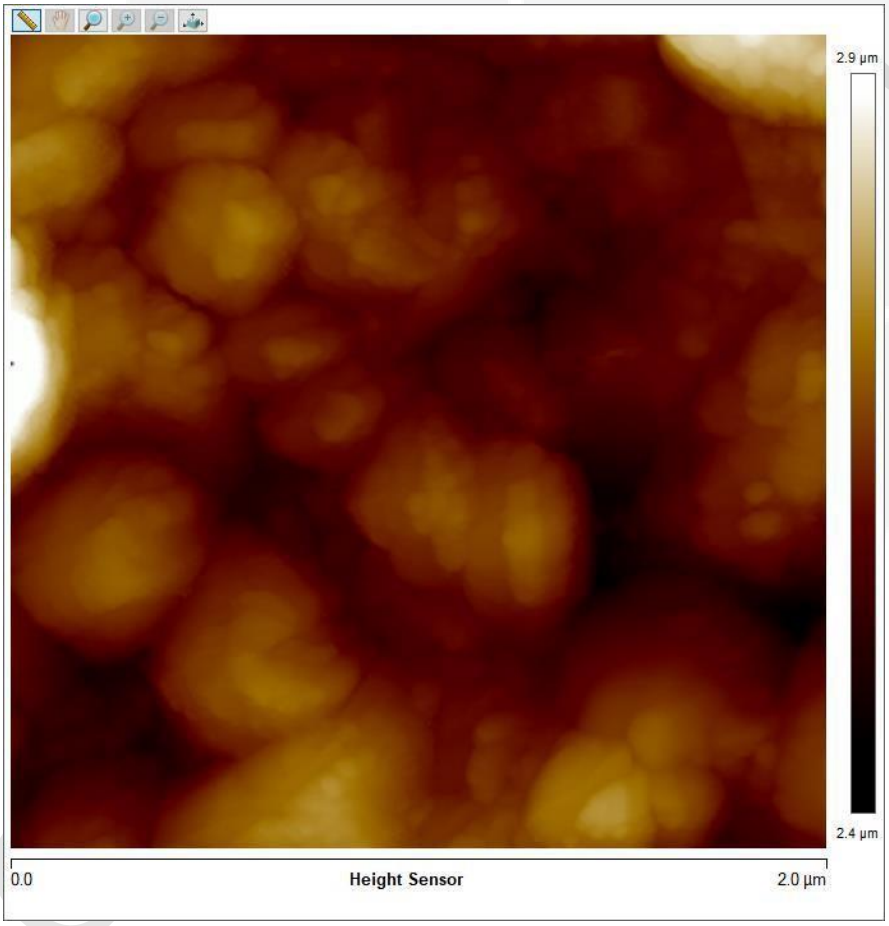

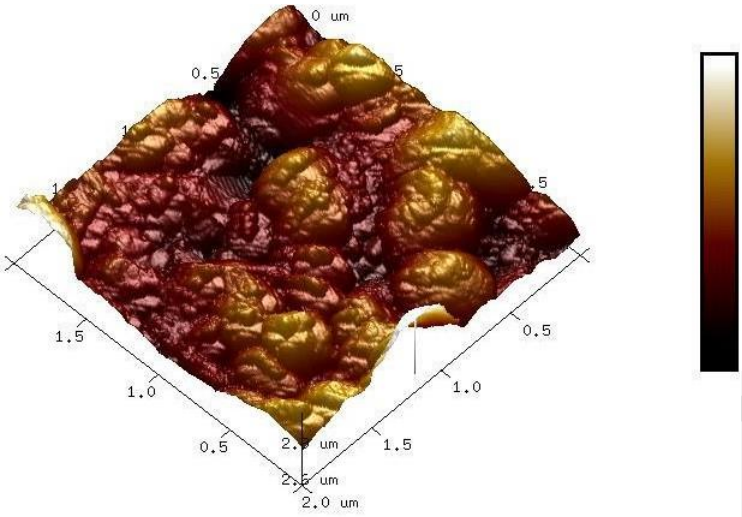

b)

Figure 4.3. AFM images on MYB06 film at different dimensions with high distribution with a peak width of 385 nm. a) 2D b) 3D

Based on Figure 4.3, ?????????????

4.2 Elemental Analysis via Energy Dispersion X-ray where is your SEM images???

Energy Dispersive Spectroscopy (EDX) analysis was carried out for all samples. Figures ?? to ?? exhibits the result of EDX analysis. The atomic percentage of the elements for each spectrum is tabulated in Table ?? to Table ??. Unfortunately, no data for MUSTO30 was able to acquire. Explain more. Please refer my thesis.

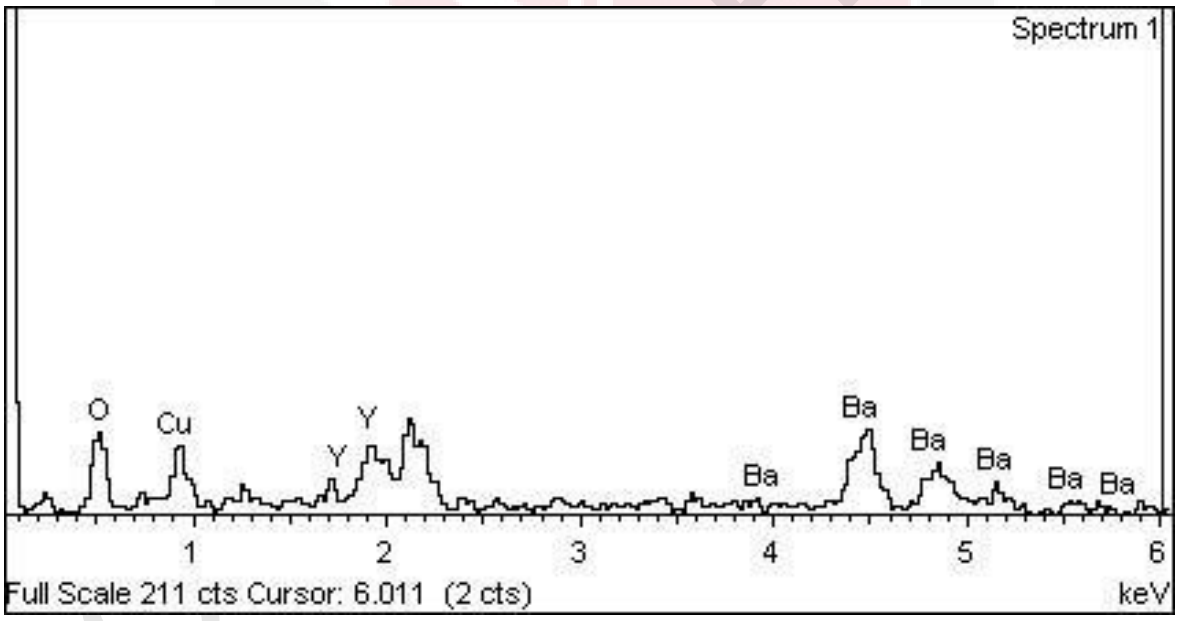

Figure 0.2. A test result of MYB006 film using EDX.

Table 4.1. Quantitative elemental analysis of MYB06 film obtained by EDS analysis

Element	Shell	Weight %	Atomic %
O	K	33.96	74.13

Cu	K	24.62	13.53
Y	L	12.97	5.09
Ba	L	28.46	7.24

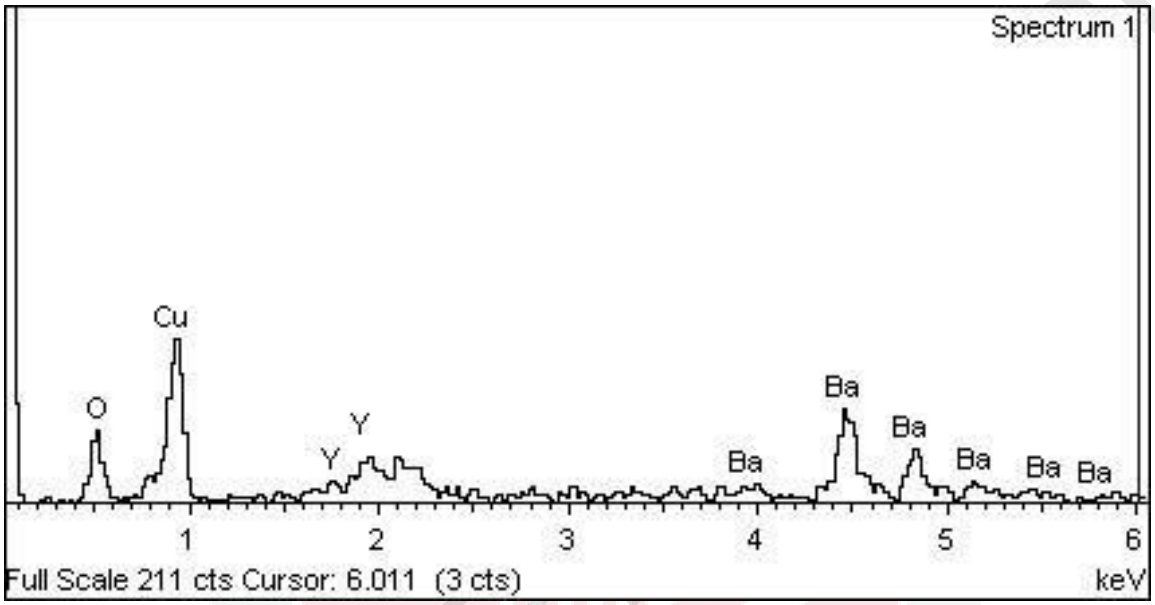

Figure 0.3. A test result of MGD001 film using EDX.

Table 4.2. Quantitative elemental analysis of MGD001 film obtained by EDS analysis

Element	Shell	Weight %	Atomic %
O	K	25.36	64.01
Cu	K	37.91	24.10
Y	L	6.79	3.08
Ba	L	29.94	8.80

4.2.1 "Type your sub tittle HERE"

"Type your subtitle paragraph HERE."

4.3 X-ray Diffraction (XRD) Analysis

XRD analysis of YBCO thin films was performed to determine the superconducting phases present in the samples and its lattice parameters. The samples are scanned at range of 20 – 80 degrees (2°Theta) and the X-ray pattern are matched with ICDD (International Centre for Diffraction Data). They undergo XRD analysis for characterization purposes. Table 4.3 shows the GOF value of MGD001, MUSTO10 and MUSTO30. Add the reference data from ICDDD library. Ask nabilah for YBCO reference list

Table 4.3. The GOF value was determined for YBCO samples

Sample	GOF (%)
MGD001	3.82233
MUSTO10	4.17311
MUSTO30	4.51981

Table 4.4 states the lattice parameter, unit cell volume and orthorhombocity of the YBCO films by using the HighScore Plus software. The lattice parameter values of the three samples are different with their respective theoretical values.

Table 4.4. The lattice parameter, unit cell volume and orthorhombocity

Sample	Lattice parameter			Unit cell volume ($Å^3$)	Orthorhombocity [(a-b)/(a+b)]
	a (Å)	b (Å)	c (Å)		
MGD001	5.50261	10.95327	3.90816	235.5512	0.33
MUSTO10	10.10219	10.10219	4.29397	379.5081	Trigonal (hexagonal axes)
MUSTO30	2.73254	7.33365	11.36734	227.7958	0.45

Table 4.5. The value of FWHM, Crystallite Size and Lattice Strain of the sample are listed in the table below.

Sample	Scherrer		
	FWHM of main peak	Crystallite size (nm)	Lattice strain (%)
MGD001	0.94464	238.3	0.147
MUSTO10	0.31488	29.2	0.794
MUSTO30	0.31488	87.4	0.271

Figure _ to _ exhibit the XRD graphs for samples MGD001, MUSTO10 and MUSTO30 respectively.

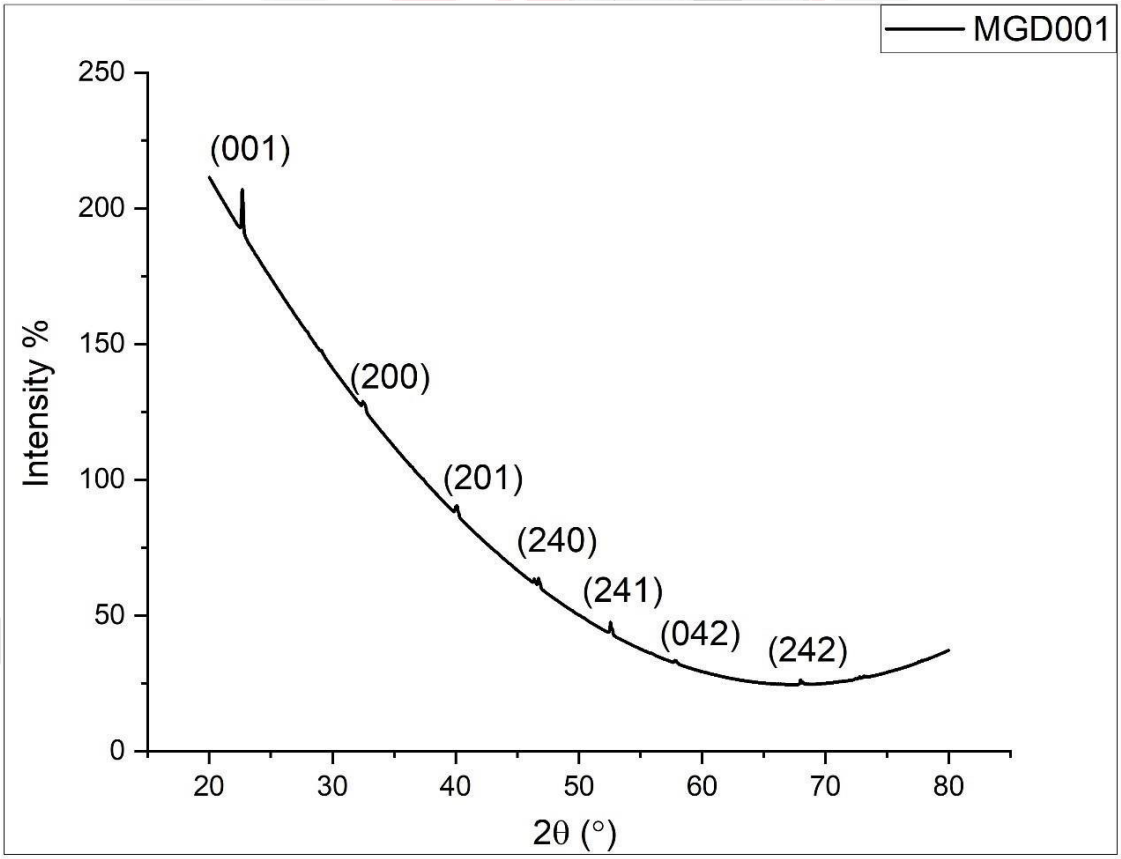

Figure 0.4. Shows the XRD graph of MGD001 film.

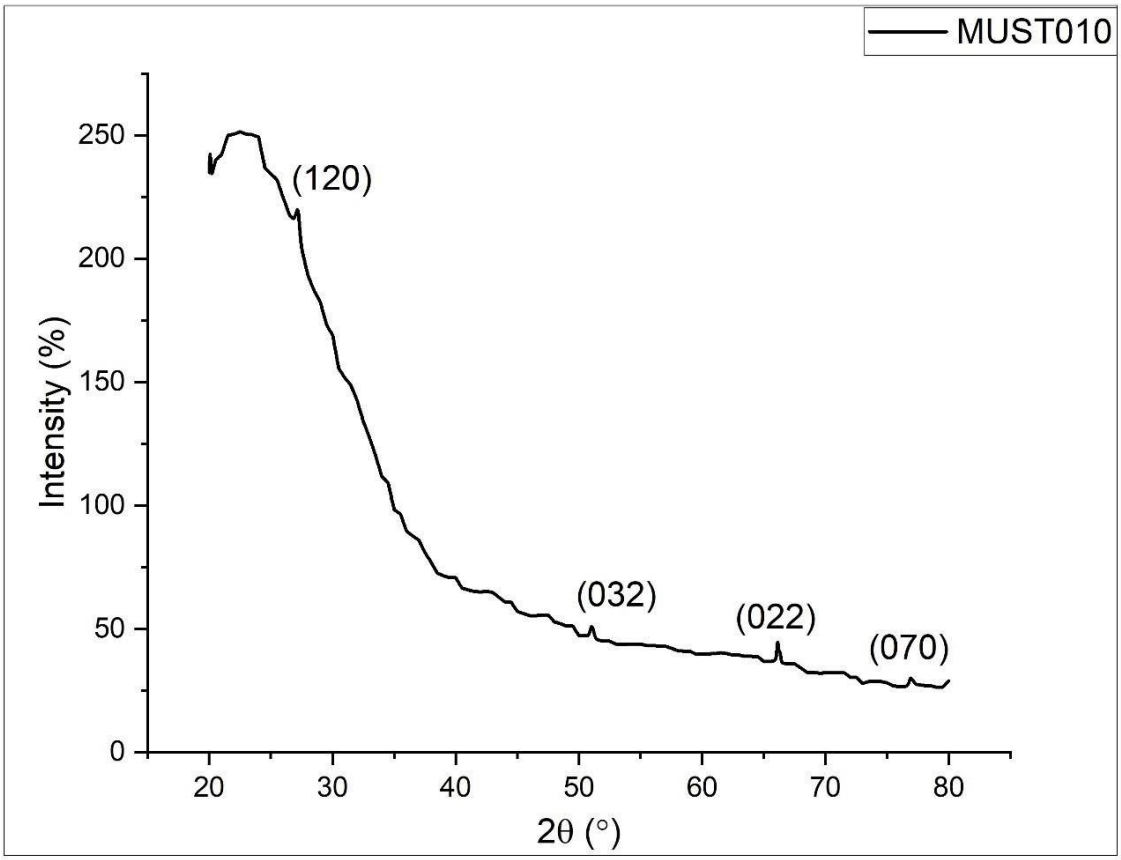

Figure 0.5. Shows the XRD graph of MUSTO10 film.

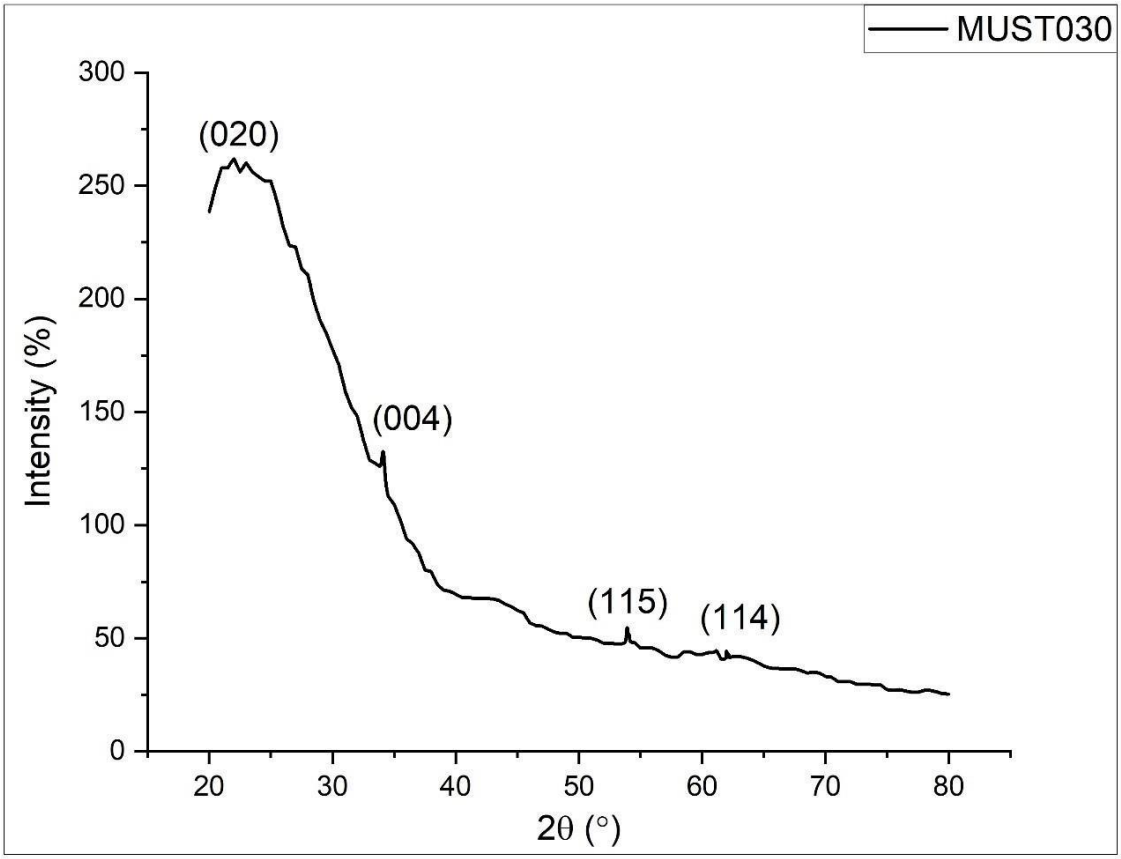

Figure 0.6. Shows the XRD graph of MUSTO30 film.

CHAPTER 5

CONCLUSION & recommendation

The YBCO thin films – MGD001, MUSTO10, MUSTO30 and MYB06 have shown that the microstructure of thin films remain the same. However, not all were able to obtain data due to its size or weakening superconducting properties, given that the samples have been kept for a decade in an enclosed cool area. MUSTO10 and MYB06 was undetectable when undergoing SEM and XRD respectively. This may be due to any defects that occur which could not be seen by the naked eye. Therefore, this occurrence should be researched in detail for the future superconductors. Too short. Describe your finding in this study such as surface roughness, surface height from AFM. The grain size from SEM images.

REFERENCES

Akmaliyah, M. (2013). 済無No Title No Title. *Journal of Chemical Information and Modeling*, *53*(9), 1689–1699.

Cheng, K. C. (1949). Theory of superconductivity [5]. *Nature*, *163*(4137), 247. https://doi.org/10.1038/163247a0

Goodstein, D., & Goodstein, J. (2000). Richard Feynman and the History of Superconductivity. *Physics in Perspective*, *2*(1), 30–47. https://doi.org/10.1007/s000160050035

Lee, H. W., Kim, K. C., & Lee, J. (2006). Review of Maglev train technologies. *IEEE Transactions on Magnetics*, *42*(7), 1917–1925. https://doi.org/10.1109/TMAG.2006.875842

Luiz, A. M. (2011). – *THEORY AND APPLICATIONS Edited by Adir Moysés Luiz*. www.intechopen.com

Module 7: High temperature Superconductors Introduction. (2012). *189*(1986).

Orthacker, A. (n.d.). *1 What is a type I and a type II superconductor? 0*(1), 1–4. http://lampx.tugraz.at/~hadley/ss2/problems/super/s.pdf

Siegrist, T., Greedan, J. E., Garrett, J. D., Wenhe, G., & Stager, C. V. (1991). Crystal structure and superconductivity in Re2Si. *Journal of The Less-Common Metals*, *171*(2), 171–177. https://doi.org/10.1016/0022-5088(91)90140-Y

APPENDICES